

ASSESSMENTS OF UNIFIED THEORIES IN SIMULATING CREEP-RATCHETTING BEHAVIOR OF VISCOUS MATERIALS

Mohammad Abdel-Karim

*Department of Mechanical Engineering
University of Maryland-Baltimore County
1000 Hilltop Circle, Baltimore, Maryland 21250, USA
Phone: (410) 455-3309 Fax:(410) 455-1052
E-mail: karim12004@yahoo.com, karim@umbc.edu*

ABSTRACT

In this work, effectiveness and capabilities of unified theories, in which creep strain and plastic strain are regarded as inelastic strain identically, are examined carefully. To achieve this target, ability of such theories in describing inelastic creep-ratchetting behavior of materials is highlighted based on numerical simulations using specific unified theory. Comparisons with experimental results for creep-ratchetting tests on 304 stainless steel at room temperature pointed out that, unified theories are restricted in describing inelastic behavior of metallic materials and they are recommended in simulating merely a certain category of loading conditions. Predominantly, unified theories are effective in simulation inelastic strain resulting from cyclic loading with non zero mean stress as long as ratio between minimum stress and maximum stress is smaller than zero, in view of the fact that influence of material viscosity on accumulated strain becomes insignificant.

Keywords: Creep-ratchetting, Viscoplasticity, Cyclic loading, Unified theories, 304 Stainless steel.

1. INTRODUCTION

Creep and ratchetting in the context of mechanical behavior refer to phenomena where materials exhibit progressive accumulation of strain under constant loading and cyclic loading, respectively. In consequence, creep and ratchetting deformation of the metallic materials have been investigated extensively however, their interaction is hardly dealt with (for example: Krempl [1979]; Ohashi et al. [1983, 1986]; Ikegami and Niitsu [1985, 1990]; Niitsu and Ikegami [1985]; Ruggles and Krempl [1989]; Yoshida et al. [1989]; Yoshida [1990, 1995]; Ohno et al. [1998]; Kawashima et al. [1999]; Mizuno et al. [2000]; Portier et al. [2000]; Zhao et al. [2001]; Yaguchi et al. [2002 a,b]; Iyer and Lissenden [2003]; Yang et al. [2003]; Feaugas and Gaudin [2004]; Yaguchi and Takahashi [in press; a, b]).

Incidentally, as a result of viscous nature of metallic materials, interaction between creep and other behaviors are examined carefully. For example, several works have been performed to investigate experimentally the interaction between tensile inelastic deformation and creep deformation (Niitsu and Ikegami [1985, 1990]; Ohashi et al. [1986]; Ruggles and Krempl [1989]). In these experiments, significant influence of creep strain on subsequent plastic flow stress under monotonic loading is highlighted. In order to simulate such inelastic deformation it is

strain identically (Niitsu and Ikegami [1990]). These unified models seem to be successful in describing such inelastic deformation especially at elevated temperature (see for example: Chaboche and Rousselier [1983]; Benallal and Marquis [1987]; Ohno and Wang [1993]; Delobella et al. [1995]; Haupt and Schinke [1996]; Portier et al. [2000]; Bari and Hassan [2000]; Abdel-Karim and Ohno [2000]; Ohno and Abdel-Karim [2000]; Iyer and Lissenden [2003]; Yaguchi et al. [2002 b]; Yaguchi and Takahashi [in press; a, b]).

Additionally, slight experiments are performed to elucidate creep-ratchetting interaction explicitly (Yoshida [1989, 1990]). In these experiments, stress controlled uniaxial creep-ratchetting tests were conducted to investigate the viscoplastic behavior of 304 stainless steel at room temperature. Difficulties in simulating ratchetting experiments even for elastic-plastic materials (no viscous effect) raise a critical question regarding the effectiveness and capabilities of unified models to be utilized in simulating such creep-ratchetting interaction tests and consequently in describing over all inelastic behavior of metallic materials.

The current work, therefore, is presented to elucidate the capabilities of unified models in predicting a benchmark test for creep-ratchetting on 304 stainless steel at room temperature performed by Yoshida and his co-workers (Yoshida et al. [1989]; Yoshida [1990]). It is shown that unified theories have enormous limitations in describing viscoplastic behavior of metallic materials and they are recommended in simulating only specific loading conditions. Particularly, unified theories are effective in simulating experiments of cyclic loading with non zero mean stress with or without peak stress hold time, on condition that ratio between minimum and maximum stresses is smaller than zero in view of the fact that effect of material viscosity on accumulated inelastic strain becomes negligible.

2. EXPERIMENTS OF YOSHIDA AND HIS CO-WORKERS [1989, 1990]

In these experiments, series of stress controlled uniaxial creep-ratchetting tests were conducted on 304 stainless steel specimens (Yoshida et al. [1989]; Yoshida [1990]). It should be noted that these experiments were carried out on the same material but the shape of the specimens were different, an hour-glass in experiments of Yoshida (1990) and straight bar in that of Yoshida et al. (1989). The stress conditions in the tests are schematically illustrated in Fig. 1 and identified in Table 1: (a) tension at constant stress rate (Yoshida, [1990]); (b) creep under constant stress (Yoshida, [1990]); (c) creep under constant stress followed by tension (Yoshida et al., [1989]); (d) cyclic loading followed by tension (Yoshida et al., [1989]); (e) creep after cyclic loading (Yoshida et al., [1989]); (f) cyclic loading after creep (Yoshida et al., [1989]); (g) cyclic loading with hold time (Yoshida et al., [1989]). In cyclic loading tests, stress ratio R is defined as ratio between minimum and maximum stresses).

It is necessary to recognize that Yoshida et al. (1989) provided experimental results with no any attempt for simulations. The new contribution of this work, therefore, represented in attempt to simulate these experiments as well as assessment of unified models in predicting such category of loading conditions. The significance of the current simulations is to identify the effectiveness of unified theories in replicating creep strain during ratchetting experiments. This is because viscous nature of material or creep is one of the driving forces for ratchetting (Krempf [1979]).

3. CONSTITUTIVE EQUATIONS AND MATERIAL PARAMETERS

First of all, it is assumed that total strain $\boldsymbol{\varepsilon}$ is divided additively to elastic part $\boldsymbol{\varepsilon}^e$ and inelastic part $\boldsymbol{\varepsilon}^i$.

$$\boldsymbol{\varepsilon} = \boldsymbol{\varepsilon}^e + \boldsymbol{\varepsilon}^i \quad (1)$$

and that the elastic part obeys Hooke's law

$$\boldsymbol{\varepsilon}^e = \frac{1+\nu}{E} \boldsymbol{\sigma} - \frac{\nu}{E} (\text{tr} \boldsymbol{\sigma}) \boldsymbol{I} \quad (2)$$

where, E and ν denote elastic constants, $\boldsymbol{\sigma}$ and \boldsymbol{I} represent stress tensor and the unit tensor of rank two, respectively, and tr the trace.

From now on and in order to avoid discrepancy, a bold letter or symbol with a tilde below represents a second order Cartesian tensor, $\boldsymbol{\sigma}$ is the stress tensor, \boldsymbol{s} is the deviatoric stress tensor, $\boldsymbol{\alpha}$ is the current center of the yield surface or back stress tensor, \boldsymbol{a} is the current center of the yield surface in the deviatoric space, and σ_0 is the size

Table 1. Classification of Experiments of Yoshida

Test	Fig	Stress Condition	Source
Tension at constant stress rate	1 (a)	$\dot{\sigma} = 0.01, 1, 30, 100$ (MPa/s)	Yoshida (1990)
Creep under constant stress	1 (b)	$\dot{\sigma} = 30$ (MPa/s)	Yoshida (1990)
Creep under constant stress followed by tension	1 (c)	$\dot{\sigma} = 12.3$ (MPa/s)	Yoshida (1989)
Cyclic loading followed by tension	1 (d)	$\dot{\sigma} = 0.25$ (MPa/s)	Yoshida (1989)
Creep after cyclic loading	1 (e)	$\dot{\sigma} = 12.3$ (MPa/s)	Yoshida (1989)
Cyclic loading after creep	1 (f)	$\dot{\sigma} = 12.3$ (MPa/s)	Yoshida (1989)
Cyclic loading with hold time	1 (g)	$\dot{\sigma} = 12.3$ (MPa/s)	Yoshida (1989)

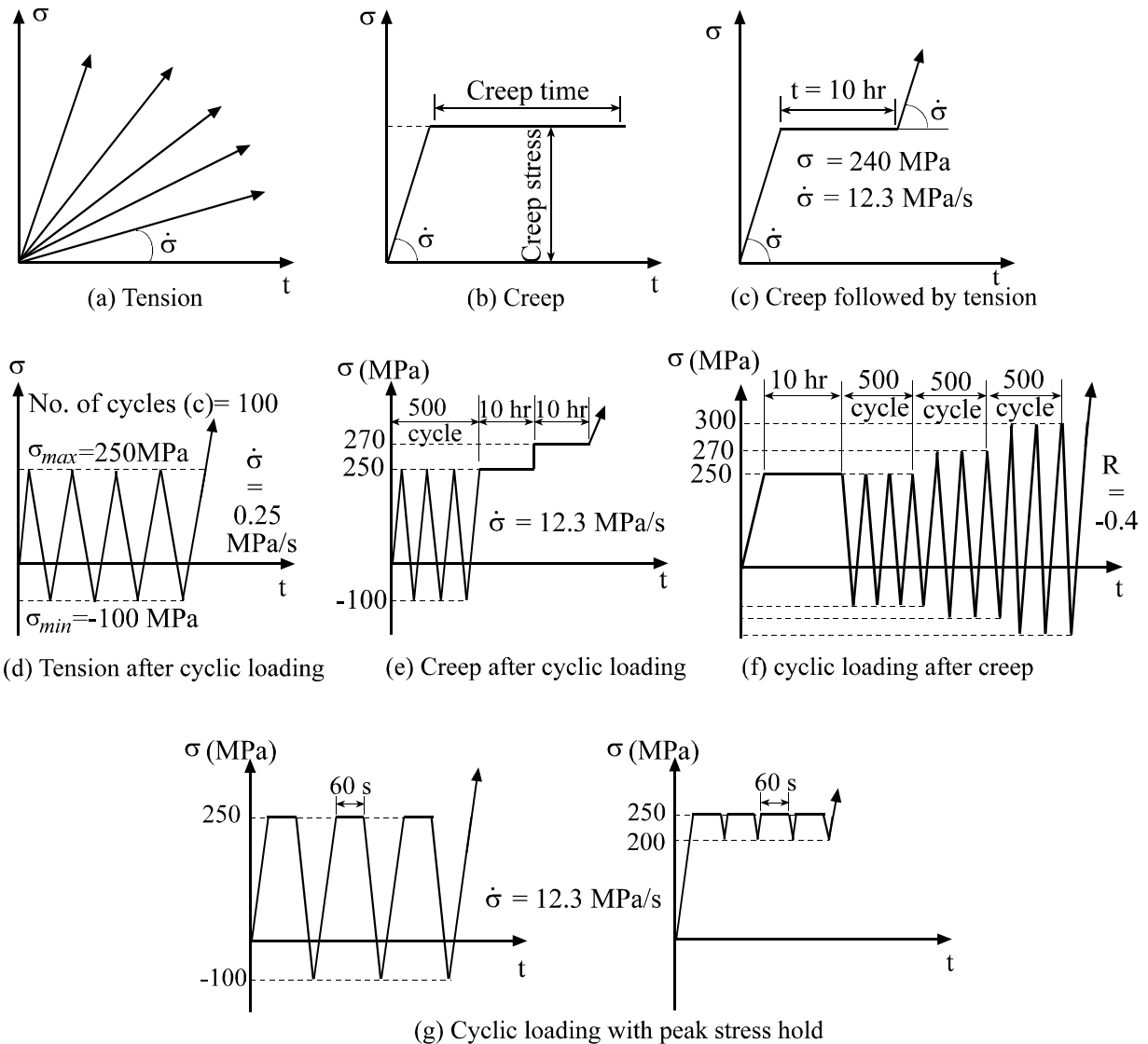


Fig. 1 Stress conditions in experiments of Yoshida

of the yield surface (constant for a cyclically stable material). Also, $\langle \rangle$ indicates the MacCauley bracket (i.e. $\langle w \rangle = (w + |w|)/2$) and the inner product $\underline{\mathbf{L}} : \underline{\mathbf{M}} = L_{ij} M_{ij}$.

According to unified theories, inelastic strain, $\underline{\boldsymbol{\varepsilon}}^i$, is regarded as plastic strain and creep strain. In these theories, over stress or viscous stress σ_v is introduced to define viscoplastic potential Ω (Chaboche and Rousselier [1983]; Benallal and Marquis [1987])

$$\Omega = \frac{A}{n+1} \langle \sigma_v \rangle^{n+1} \quad (3)$$

here A and n are material constants and over stress σ_v is defined as

$$\sigma_v = J(\sigma - \alpha) - \sigma_0 \quad (4)$$

$$J(\sigma - \alpha) = \sqrt{\frac{3}{2} (\underline{\boldsymbol{s}} - \underline{\boldsymbol{a}}) : (\underline{\boldsymbol{s}} - \underline{\boldsymbol{a}})} \quad (5)$$

hence, σ_0 refers to the initial yield stress under quasi-static loading, $\underline{\boldsymbol{s}}$ and $\underline{\boldsymbol{a}}$ are deviatoric parts of stress tensor $\underline{\boldsymbol{\sigma}}$ and back stress $\underline{\boldsymbol{\alpha}}$, respectively. It is noted that, for 304 stainless steel, isotropic hardening effect is almost negligible as long as strain range is relatively small (Yoshida [1990]). Therefore, this effect is neglected in this work. Then inelastic strain $\underline{\boldsymbol{\varepsilon}}^i$ is obtained from flow rule as

$$\dot{\underline{\boldsymbol{\varepsilon}}}^i = \frac{\partial \Omega}{\partial \underline{\boldsymbol{\sigma}}} = \frac{3}{2} A \langle \sigma_v \rangle^n \frac{\underline{\boldsymbol{s}} - \underline{\boldsymbol{a}}}{J(\sigma - \alpha)} \quad (6)$$

To complete constitutive equations, evaluations rules for back stress $\underline{\boldsymbol{\alpha}}$, are introduced as

$$\underline{\boldsymbol{\alpha}} = \sum_{j=1}^M \underline{\boldsymbol{\alpha}}_j \quad (7)$$

$$\dot{\underline{\boldsymbol{\alpha}}}_j = \zeta_j \left(\frac{2}{3} r_j \dot{\underline{\boldsymbol{\varepsilon}}}^p - H(f_j) \left\langle \dot{\underline{\boldsymbol{\varepsilon}}}^p : \frac{\underline{\boldsymbol{a}}_j}{\bar{a}_j} \right\rangle \underline{\boldsymbol{a}}_j \right) \quad (8)$$

where, $\underline{\boldsymbol{a}}_j$ is the deviatoric part of back stress component $\underline{\boldsymbol{\alpha}}_j$, ζ_j and r_j ($j=1,2,\dots,M$) are material constants, H stands for Heaviside's step function (i.e., $H(x)=1$ if $x \geq 0$ and $H(x)=0$ if $x < 0$), $f_j = \bar{a}_j^2 - r_j^2$, $\bar{a}_j = [(3/2) \underline{\boldsymbol{a}}_j : \underline{\boldsymbol{a}}_j]^{1/2}$ and $\langle \rangle$ represents MacCauley's bracket (Ohno and Wang [1993]). The above equation is identical to kinematic hardening rules proposed by Ohno and Wang [1993]. It is noticed that these rules provide complete closure of stress strain hysteresis loops under uniaxial cyclic loading with non zero mean stress resulting in no uniaxial ratchetting except for viscosity effect.

At the end of this part, the material parameters shown in Table 2 were determined on the basis of the uniaxial monotonic tensile experiments at different stress rates shown in Fig. 2.

Table 2. Material parameters for 304 stainless steel

$r_1 = 12, \zeta_1 = 10000$	$r_6 = 13, \zeta_6 = 180$
$r_2 = 14, \zeta_2 = 5000$	$r_7 = 5, \zeta_7 = 100$
$r_3 = 15, \zeta_3 = 2500$	$r_8 = 9, \zeta_8 = 50$
$r_4 = 15, \zeta_4 = 1000$	$r_9 = 9, \zeta_9 = 30$
$r_5 = 15, \zeta_5 = 400$	$r_{10} = 80, \zeta_{10} = 20$

$$A = 5.0E - 24, \quad n = 10.5, \quad \sigma_0 = 50, \quad E = 194000$$

Stress (MPa), strain (mm/mm), time

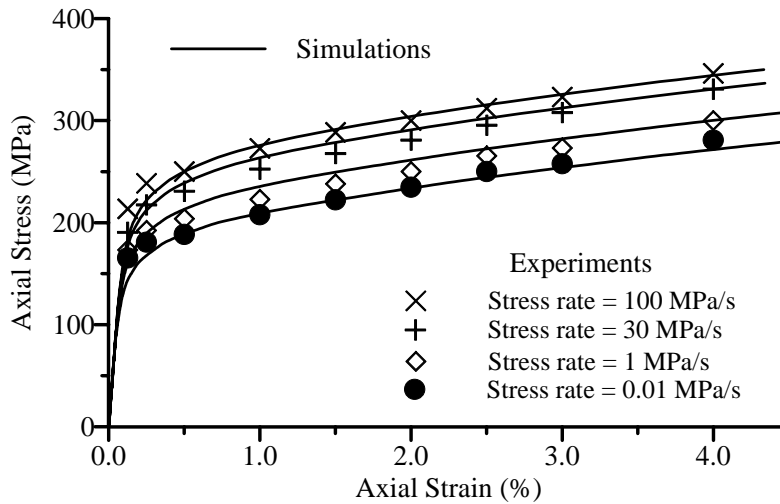
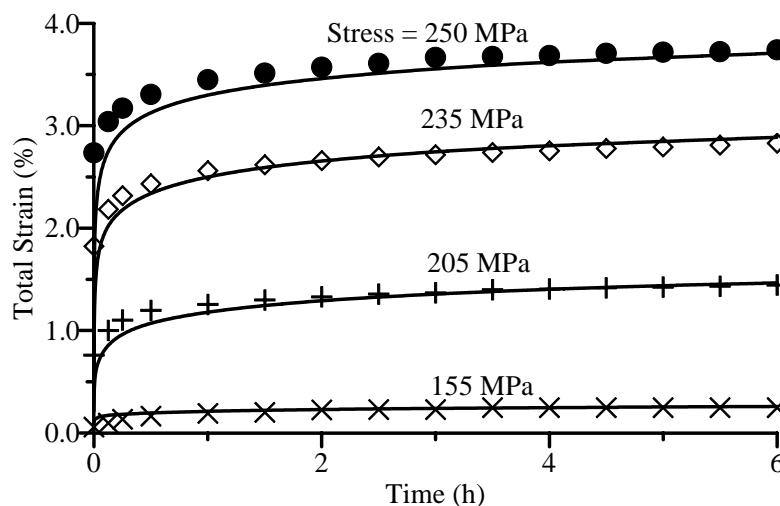


Fig. 2 Tensile stress strain curves at constant stress rates for 304 stainless steel

4. APPLICATIONS TO EXPERIMENTS AND DISCUSSIONS

Simulations of different loading conditions shown in Fig. 1 using aforementioned model based on unified theory is compared with experiments. The results of simulations along with experimental data are represented in Figs. 2 through 8. It should be emphasized that symbols indicated in these figures (especially those in Figs 4-8) represent experimental strain value corresponding to tested stress level.

First of all let us consider classical loading conditions, i.e. tension at constant stress rate and creep under constant stress illustrated in Figs. 1 a&b. As a matter of fact, the material constants used in the current work and shown in Table 2 are determined mainly to simulate experimental data of tension tests at constant stress rate shown in Fig. 2. Thus the model simulates these tests well as indicated in the figure. With respect to simulations of creep tests, Fig. 3, it is clear that such unified model can successfully predict creep strain fairly well especially at lower values for stress and accuracy of simulation tends to decrease with increasing creep stress. The reasons behind this behavior will be discussed latter. Moreover, we should remember that, these creep tests are performed at one of the loading rate conditions at which utilized material parameters are determined. This point is also clarified later on.



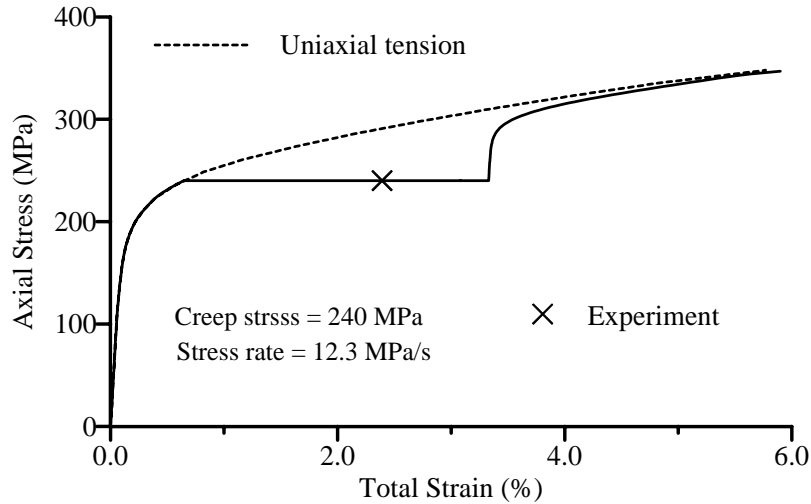


Fig. 4 Simulation of creep followed by tension

Now let us deal with atypical test, i.e. creep under constant stress followed by tension. The predicted stress strain response is compared with experiment results in Fig. 4. The symbol in the figure represents experimental strain value at the end of the creep test. In this case, experimental trend is simulated well since, stress strain curve in the tension part subsequent to creep reaches monotonic stress strain curve (Yoshida [1990]). However, it is evident that, the predicted strain value during creep is relatively greater than experimental results. This is in contrast with creep tests shown in Fig. 3 in which experiments are simulated well at different creep stress. The reason behind these unaccepted results can be attributed to the value of loading rate. Since utilized loading rate value ($\dot{\sigma} = 12.3$ MPa/s) is not one of the loading rate conditions shown in Fig. 2 at which material parameters are determined. In other words utilized viscous function is effective merely at value of loading conditions at which material parameters are obtained. Actually, the calculated stress-strain responses by any constitutive models are directly influenced by chosen material parameters. In unified constitutive modeling, however, this influence is significantly observed and this significant effect can be attributed mainly to the viscous part introduced in the model.

It should be noted that, ultimately, the two curves shown in Fig. 4 usually merge for 304 stainless steel as indicated by Yoshida et al. (1989). This feature is also pointed out in uniaxial experiments of 316FR steel at room temperature (Mizuno et al. [2000]). Actually Yoshida defined this behavior to be a measure for work-hardening of 304SS (Yoshida et al. [1989]). On the other hand, for 316FR steel, it is attributed to the complete closure of stress strain hysteresis loops and negligible influence of isotropic hardening as long as strain range is relatively small (Mizuno et al. [2000]). From the simulation point of view, this feature can be simulated well using unified theories without consideration for creep ratchetting interaction since it is pure creep problem.

Simulation of cyclic loading followed by tension in comparison with value of experimental strain at the end of 100th cycles is shown in Fig. 5. In this case, its is also clear that the subsequent tension part tends to coincide with monotonic one after stress cycles, the feature which is observed experimentally (Yoshida [1990]). The important feature in this test is the value of accumulated strain during ratchetting. It is clear the model provides ratchetting strain and this value is relatively higher than experiments. In this case the predicted strain is mainly due to viscous effect, which is somewhat, is active since kinematic hardening rule provide no uniaxial ratchetting. However, any additional strain resulting from kinematic hardening rules leads to higher strain. Therefore poor representation for this test can be also attributed to limitation in simulating viscous effect described by unified theory.

With respect to test of creep after cyclic loading, interaction between creep and ratchetting will be more obvious. Figure 6 illustrates predictions of strain in comparison with experimental results. In this figure, it is necessary to differentiate between ratchetting strain and creep strain. Therefore strain obtained from each part is separately compared with experiments. It is obvious that, during cyclic loading part, the model underestimates experimental

utilized kinematic hardening rules provide complete closure of stress strain hysteresis loops, i.e. no uniaxial ratchetting is allowed except for viscous effect. Thus ratchetting strain can be simulated well if very small opening is assumed for stress strain hysteresis loops. Consequently, such small opening, the feature that is observed in 316FR steel (Mizuno et al. [2000]), increases ratchetting strain and experimental results can be simulated well. However, it should be recognized that, even very small for stress-strain hysteresis loops resulting in further increase in subsequent creep strain. In other words, unified theory fails also in simulating creep strain subsequent to ratchetting tests. Therefore, we can conclude that loading sequence has no influence on the predicted results. Moreover, unified theory can simulate ratchetting strain well under certain conditions but it tends to overestimate creep strain subsequent to ratchetting.

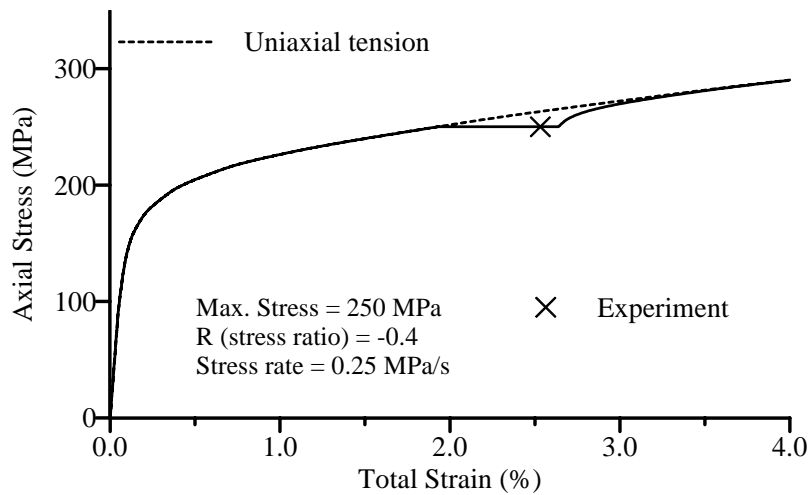


Fig. 5 Simulation of cyclic loading followed by tension

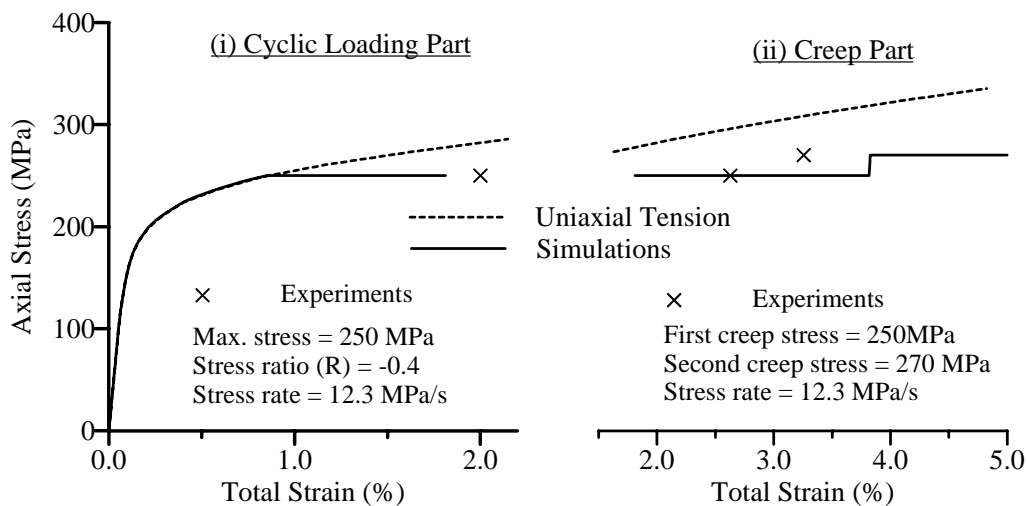
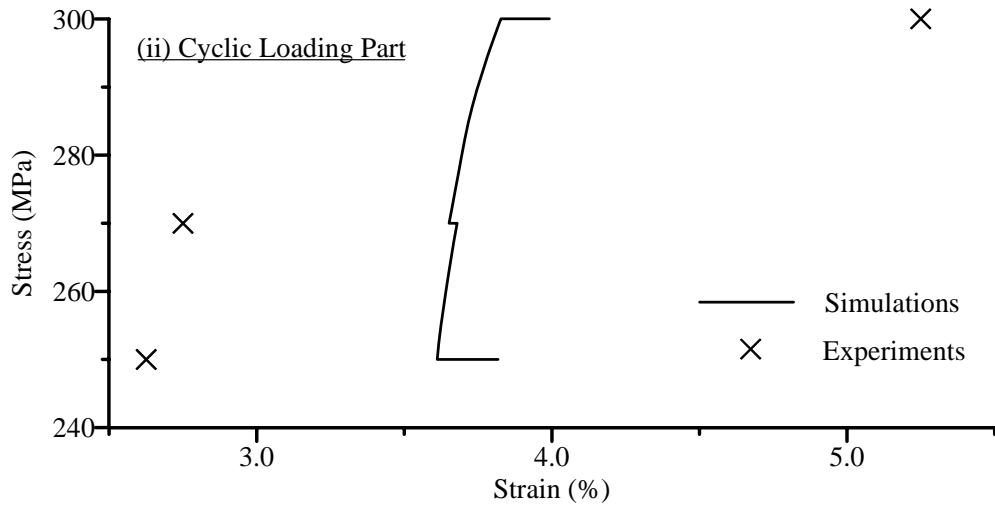
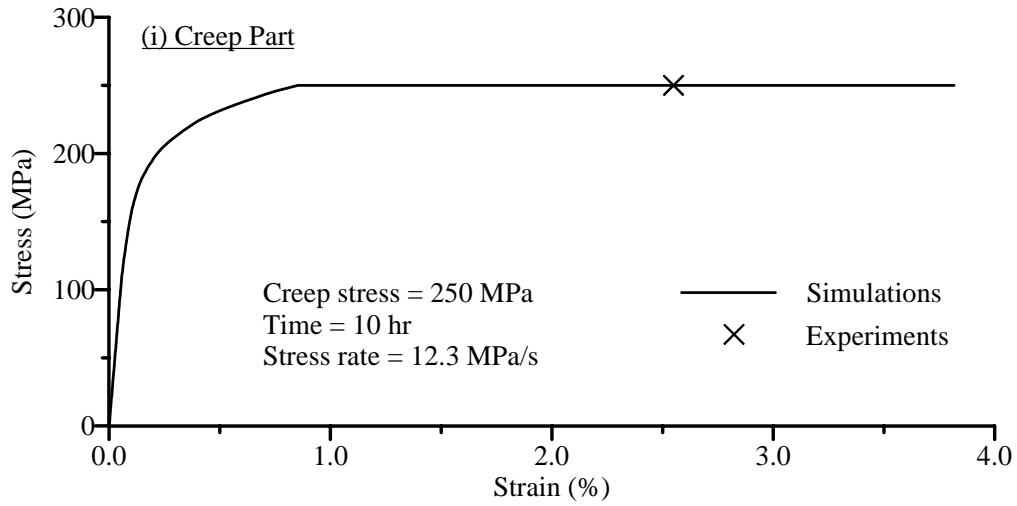
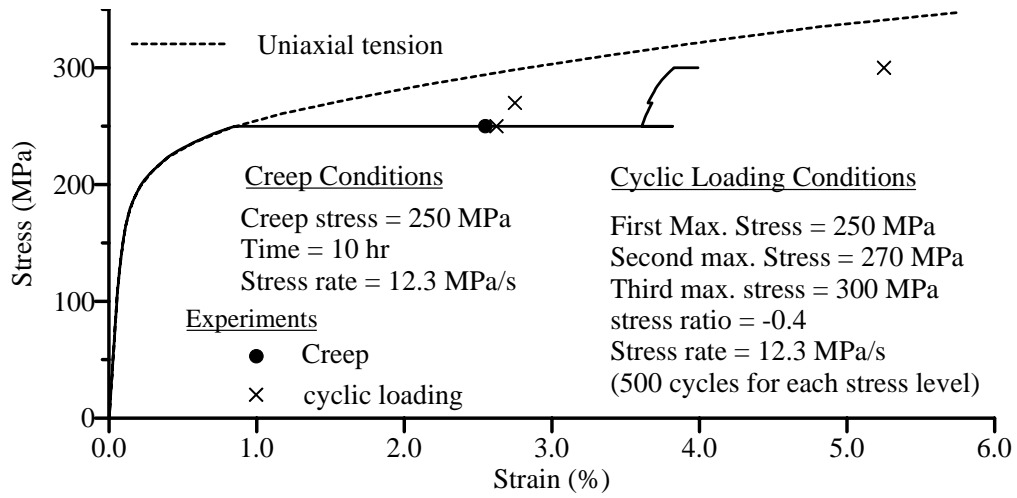
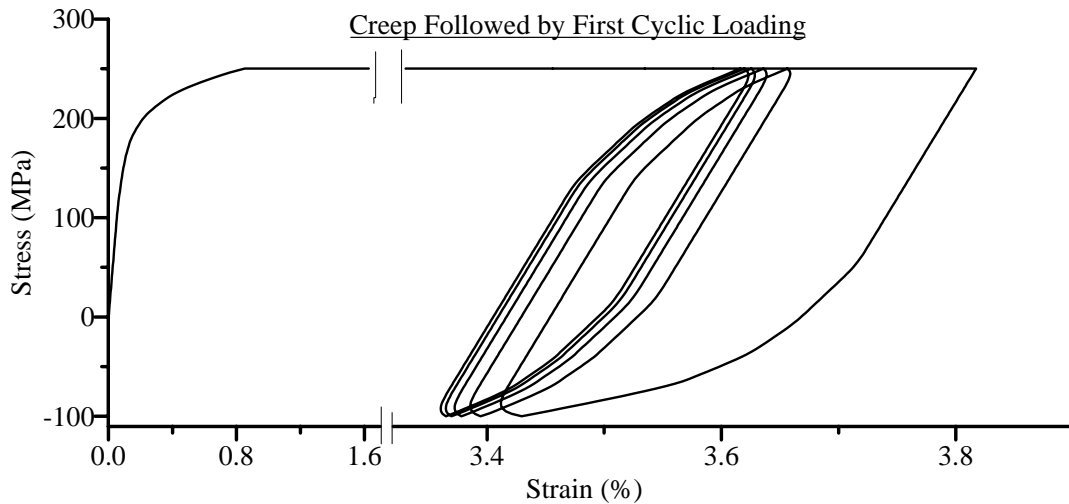


Fig. 6 Simulation of creep subsequent to cyclic loading (symbols refers to experimental values by



(a) Stress strain relation

Fig. 7 Simulation of creep followed by cyclic loading (symbols refers to experimental values by



(b) Stress strain hysteresis loops during first cyclic loading after creep

Fig. 7 Continued

Additional observations are obtained by simulations for creep subsequent to ratchetting test shown in Figs. 7 a&b. It is evident that the predicted creep strain is greater than experiments, Fig. 7i. Hence it seems that the unified theory is affected not only by loading rate but also is affected by total creep period. In this test, creep period is equal to ten hours while it was only six hours in simulations exposed in Fig. 3. This result indicates that accuracy of simulations of creep strain using unified theory could be highly affected by value of total period of creep test. Moreover, model fails not only to simulate creep strain but also to simulate experimental trend during first and second subsequent ratchetting (Fig. 7ii). Hence negative ratchetting strain is predicted in both of them in contrast with experimental results, which provides a little ratchetting strain in each subsequent cyclic loading. In addition, the model provides a little ratchetting strain during third subsequent ratchetting in contrast with experiments in which notable ratchetting strain is obtained (Fig. 7ii).

The reason behind this discrepancy can be clarified with the aid of Fig. 7b, which illustrate variation of stress strain hysteresis loops during first subsequent cyclic loading. It is clear that, the stress strain hysteresis loops move in negative direction although maximum stress value is positive. This is because the first subsequent cyclic loading test is performed with the same value of creep stress (maximum stress = 250 MPa). Consequently, the large accumulated creep strain causes too much activation for dynamic recovery of kinematic hardening rules, which leads to negative ratchetting strain under successive cyclic loading with the same maximum stress value. Hence, during creep test, the change in stress increment ($\dot{\sigma}$) is equal to zero while back stress changes continuously due to viscous effect. As a result difference ($\sigma - \alpha$) decreases. During consequent cyclic stressing and since maximum stress is the same, the difference ($\sigma - \alpha$) decreases further and negative value will be obtained resulting in negative inelastic strain. In addition, negative ratchetting strain (almost negligible) during second subsequent cyclic loading (maximum stress = 270 MPa) can be ascribed to the same reasons; hence change in maximum stress value is relatively small to overcome initial creep strain or to provide positive value for difference ($\sigma - \alpha$). When change in maximum stress becomes relatively large and difference ($\sigma - \alpha$) becomes positive, positive ratchetting strain is predicted, i.e. during third later cyclic loading.

To end with, simulations for cyclic loading with hold time are illustrated in Fig. 8. In this figure, predicted results for static creep are also illustrated for the sake of comparison. It is clear that predicted results from this creep test is almost identical to the predicted results of cyclic loading with peak-stress hold test as stress ratio $R=0.8$ ($R = \text{minimum stress}/\text{maximum stress}$). On the other hand, when $R=-0.4$ the difference becomes notable and the steady state response for variation of accumulated strain is predicted. The reasons behind this tendency can be for

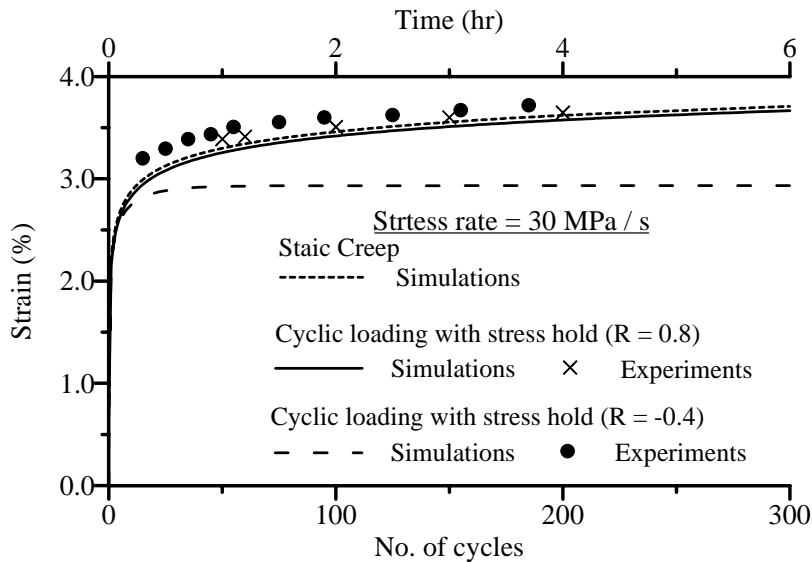


Fig. 8 Simulations of cyclic loading with peak stress hold time

the most part explained as follows: When $R = 0.8$, viscous effect prevails on material behavior and the predicted strain is mainly attributed to creep strain that obtained during hold time. Thus, stress strain curve is almost identical to that of creep test. When $R = -0.4$, i.e. stress ratio is smaller than zero, ratchetting strain prevails and influence of both material viscosity and hold time and consequently creep strain acquired by unified theory is almost negligible except for first few cycles.

The current study has pointed out some drawbacks of unified models. As a matter of fact, although unified theories are widely used and provide very good results in many loading conditions as mentioned in the introductory section, the mentioned drawbacks can be considered as specific problems in unified modeling as long as power law is assumed to describe viscous effect irrespective of utilized kinematic and/or isotropic hardening rules. To generalize these drawbacks, however, more extensive study considering different forms capable of describing viscous effect should be considered.

5. CONCLUSIONS

- Effectiveness and capabilities of unified theories in simulating inelastic behavior of ratchetting-creep behavior for metallic materials are carefully examined.
- Unified models can simulate qualitatively uniaxial loading subsequent to creep or cyclic loading. However, they fail in simulating creep subsequent to cyclic loading or cyclic loading subsequent to creep. In these experiments, it is not sufficient to consider only uniaxial tensile tests at different strain rate to replicate viscosity effect.
- The calculated stress-strain responses by any constitutive models are directly influenced by chosen material parameters. In unified theories, however, this influence is significantly observed and this significant effect can be attributed mainly to the viscous part introduced in the theory
- Unified theories are recommended in simulating experiments in which viscous effect is relatively small. Particularly, simulations of inelastic strain resulting from cyclic loading with non zero mean stress with or without hold time as long as ratio between minimum stress and maximum stress is smaller than zero.
- The aim of the current work is to assess the unified theories as it was with no attempt to model experiments. To achieve the goal of predicting deformation behavior under stress boundary conditions including cyclic loading effect of initial conditions and loading sequence should be encountered. A consistent work on these subjects is needed and will be considered in forth coming work.
- The results obtained in this work are based on a specific type for viscous function. In order to generalize these results, more extensive study considering different functions is necessary.

REFERENCES

- Abdel-Karim, M., Ohno, N., (2000). *Int. J. of Plasticity*, Vol. 16, No. 3-4, pp. 225-240.
- Bari, S., Hassan, T., (2000). *Int. J. of Plasticity* Vol. 16, No. 3-4, pp. 381-410.
- Benallal, A., Marquis, M., (1987). *ASME, J. Eng. Mat. Tech.* Vol. 109, No. 4, pp. 326-336.
- Chaboche, J.L., Rousselier, G., (1983). *ASME, J. Press. Vessel and Tech.*, Vol. 108, No. 3, pp. 153-164.
- Delobella, P., Robinet, P., Bocher, L., (1995). *Int. J. of Plasticity*, Vol. 11, No. 4, pp. 295-330.
- Feaugas, X., Gaudin, C., (2004). *Int. J. of Plasticity*, Vol. 20, No. 4-5, pp. 643-662.
- Haupt, A., Schinke, B., (1996). *ASME J. Eng. Mat. And Tech.*, Vo. 118, No. 3, pp. 281-283.
- Ikegami, K., Niitsu, Y., (1985). *Int. J. of Plasticity*, Vol. 1, No. 3, 331-345.
- Iyer, S.K., Lissenden, C.J., (2003). *Int. J. Plasticity*, Vol. 19, No. 12, 2055-2081.
- Kawashima, F., Ishikawa, A., Asada, Y., (1999). *Nuclear Eng. and Design*, Vol. 193, No. 3, pp. 327-336.
- Krempf, E., 1979. *J. Mech. and Phys of solids*, Vol. 27, No. 5-6, pp.363-375.
- Mizuno, M., Mima, Y., Abdel-Karim, M., Ohno, N., (2000). *ASME J. Eng. Mat. and Tech.*, Vol. 122, No. 1, pp. 29-34
- Niitsu, Y., Ikegami, K., (1985). *Bulletin of JSME*, Vol. 28, pp. 1853-1858.
- Niitsu, Y., Ikegami, K., (1990). *ASME J. Press. Vessel and Tech.* Vol. 112, No. 2, pp. 152-157.
- Ohashi, Y., Kawai, M., Momose, T., (1986). *ASME J. Eng. Mat. and Tech.*, Vol. 108, No. 1, pp. 68-73.
- Ohashi, Y., Kawai, M., Shimizu, H., (1983). *ASME J. Eng. Mat. and Tech.*, Vol. 105, No. 3, pp. 257-263
- Ohno, N., Wang, J.-D., (1993). *Int. J. of Plasticity*, Vol. 9, No. 3, pp. 375-403.
- Ohno, N., Abdel-Karim, M., Kobayashi, M., Igari, T., (1998). *Int. J. of Plasticity*, Vol. 14, No. 4-5, pp. 355-372.
- Ohno, N., Abdel-Karim, M., (2000). *ASME J. Eng. Mat. and Tech.*, Vol. 122, No. 1, pp. 35-41.
- Portier, L., Calloch, S., Marquis, D., Geyer, P., (2000). *Int. J. of Plasticity*, Vol. 16, No. 3-4, pp. 303-335.
- Ruggles, M.B., Krempf, E., (1989). *ASME J. Eng. Mat. and Tech.*, Vol. 111, No. 4, pp. 378-383.
- Yaguchi, M., Yamamoto, M., Ogata, T., (2002a). *Int. J. of Plasticity*, Vol. 18, No. 8, pp. 1083-1109.
- Yaguchi, M., Yamamoto, M., Ogata, T., (2002b). *Int. J. of Plasticity*, Vol. 18, No. 8, pp. 1111-1131.
- Yaguchi, M., Takahashi, Y., (2005). *Int. J. of Plasticity*, Vol. 21, No. 1, pp. 43-65.
- Yaguchi, M., Takahashi, Y., (2005). *Int. J. of Plasticity*, Vol. 21, No. 4, pp. 835-860.
- Yang, X.J., Chow, C.L., Lau, K.J., (2003). *Int. J. of Fatigue*, Vol. 25, No. 6, 533-546.
- Yoshida, F., Kondo, J., Kikuchi, Y., (1989). *JSME International Journal*, Vol. 32, No. 2, 136-141.
- Yoshida, F., (1990). *Int. J. Press. Vessels and Piping*, Vol. 44, No. 2, pp. 207-223.
- Yoshida, F., (1995). *European J. Mech. A/Solids*, Vol. 14, No. 1, pp. 97-114.
- Zhao, L.G., Tong, J., Vermeulen, B., Byrne, J., (2001). *Mechanics of Materials*, Vol. 33, No. 10, pp. 593-600.